
CF-VAE: Causal Disentangled Representation Learning with VAE and Causal Flows

Di Fan

School of Mathematical Sciences
Zhejiang University
22135091@zju.edu.cn

Yannian Hou

School of Mathematical Sciences
Zhejiang University
12235044@zju.edu.cn

Chuanhou Gao

School of Mathematical Sciences
Zhejiang University
gaochou@zju.edu.cn

Abstract

Learning disentangled representations is important in representation learning, aiming to learn a low dimensional representation of data where each dimension corresponds to one underlying generative factor. Due to the possibility of causal relationships between generative factors, causal disentangled representation learning has received widespread attention. In this paper, we first propose a new flows that can incorporate causal structure information into the model, called causal flows. Based on the variational autoencoders(VAE) commonly used in disentangled representation learning, we design a new model, CF-VAE, which enhances the disentanglement ability of the VAE encoder by utilizing the causal flows. By further introducing the supervision of ground-truth factors, we demonstrate the disentanglement identifiability of our model. Experimental results on both synthetic and real datasets show that CF-VAE can achieve causal disentanglement and perform intervention experiments. Moreover, CF-VAE exhibits outstanding performance on downstream tasks and has the potential to learn causal structure among factors.

1 Introduction

Representation learning aims to learn a representation of data that allows for easier extraction of useful information when constructing classifiers or other predictors [1]. Disentangled representation learning is an important step towards better representation learning. It assumes that high-dimensional data is generated by low-dimensional, semantically meaningful factors, called ground-truth factors. Thus, disentangled representation learning refers to learning a representation where changes in one dimension are caused by only one factor of variation in the data [2]. The common framework for obtaining disentangled representations is the Variational Autoencoder (VAE) [3], which is a generative model. It uses an encoder to map data \mathbf{x} to a latent variable space, obtaining a latent variable representation \mathbf{z} .

In recent years, many unsupervised methods using VAE to learn disentangled representations have been proposed, mainly by imposing independent constraints on the posterior or aggregate posterior of latent variable \mathbf{z} through KL divergence [4–10]. Later, Locatello et al. [2] proposed that it is almost impossible to achieve disentanglement in an unsupervised manner without inductive bias. Therefore, some weakly supervised or supervised methods were proposed, such as using a supervised loss [11, 12], a conditional prior [13, 14], or paired training data [15], and the model can also achieve

parameter identifiability [14]. However, most of them assume that the generative factors of data are independent of each other, while in the real world, the generative factors of interest are likely to have causal relationships with each other. At this point, the above models cannot achieve disentanglement of causally related factors [12, 16]. In order to achieve the purpose of causal disentanglement, many state-of-the-art methods have been proposed [12, 13, 17–19], where consistency between latent variables and generative factors can be achieved by imposing a Structured Causal Model (SCM) [20] on the prior and using a loss term that incorporates supervised information as in [12]. We also incorporate similar prior information into our model to achieve this alignment.

Normalizing flows [21] is a common method for improving the inference ability of VAE, by composing a series of reversible transformations with simple Jacobian determinants, making the posterior distribution of VAE closer to the true posterior distribution. One of the most popular normalizing flows is the autoregressive flows [22], and its application combined with VAE is the Inverse Autoregressive Flows (IAF) [23]. The causal order of the model can be learned using autoregressive flows [24]. Inspired by this application, we develop a flow model that can impose arbitrary causal structures on the variables to be fitted, based on the characteristic of autoregressive flows. This enables the VAE, when combined with the flows model, to effectively leverage the causal structure information of the underlying factors and achieve causal disentanglement.

In this paper, we introduce causal flows that incorporate causal structure information of variables, and propose a causal disentanglement model based on VAE, called the CF-VAE model, which allows us to capture the relationship between the latent variable representation and the latent variables of interest. The causal matrix is introduced by treating the variable order of the autoregressive flows as the causal order, and we express the true causal structure between latent factors into the autoregressive flows by using a causal matrix. After encoding the input data and processing it through the causal flows, we obtain the causal latent variable representation, which is then fed into the decoder for the reconstruction of the original image. To guarantee the causal disentanglement of the model, we also include supervised information about the underlying factors.

The contributions of our work are as follows:

- (1) We introduce the causal flows, an improved autoregressive flows that integrates the causal structure information of variables.
- (2) We propose a new VAE model, CF-VAE, which employs the causal flows to learn a causal disentangled representation.
- (3) We show theoretically that CF-VAE can achieve the disentanglement identifiability¹.
- (4) We empirically show that CF-VAE can achieve causal disentanglement and perform intervention experiments on both synthetic and real datasets. Our model exhibits excellent performance in terms of sampling efficiency in downstream tasks, and further experiments indicate its potential to learn the causal structure.

2 Background

2.1 Variational Autoencoders

Let $\{\mathbf{x}_j\}_{j=1}^N$ denote i.i.d training data, $\mathbf{x} \in \mathbb{R}^n$ be the observed variables and $\mathbf{z} \in \mathbb{R}^d$ be the latent variables. The dataset \mathcal{X} has an empirical data distribution denoted as $q_{\mathcal{X}}$. The *generative model* defined over \mathbf{x} and \mathbf{z} is $p_{\theta}(\mathbf{x}, \mathbf{z}) = p(\mathbf{z})p_{\theta}(\mathbf{x}|\mathbf{z})$, where θ is the parameter of the *decoder*. Typically, $p(\mathbf{z}) = N(0, \mathbf{I})$, $p_{\theta}(\mathbf{x}|\mathbf{z}) = N(f_{\theta}(\mathbf{z}), \sigma^2 \mathbf{I})$, where $f_{\theta}(\mathbf{z})$ is a neural network. Then, the marginal likelihood $p_{\theta}(\mathbf{x}) = \int p_{\theta}(\mathbf{x}, \mathbf{z})d\mathbf{z}$ is intractable to maximize. Therefore, VAE [3] introduces a parametric *inference model* $q_{\phi}(\mathbf{z}|\mathbf{x}) = N(\mu_{\phi}(\mathbf{x}), \text{diag}(\sigma_{\phi}^2(\mathbf{x})))$, also called an *encoder* or *recognition model*, to obtain the variational lower bound on the marginal log-likelihood, i.e., the Evidence Lower BOund (ELBO):

$$\begin{aligned} \text{ELBO}(\phi, \theta) &= \mathbb{E}_{q_{\mathcal{X}}} [\log p_{\theta}(\mathbf{x}) - D_{\text{KL}}(q_{\phi}(\mathbf{z}|\mathbf{x})||p_{\theta}(\mathbf{z}|\mathbf{x}))] \\ &= \mathbb{E}_{q_{\mathcal{X}}} [\mathbb{E}_{q_{\phi}(\mathbf{z}|\mathbf{x})} (\log p_{\theta}(\mathbf{x}, \mathbf{z}) - \log q_{\phi}(\mathbf{z}|\mathbf{x}))] \\ &= \mathbb{E}_{q_{\mathcal{X}}} [\mathbb{E}_{q_{\phi}(\mathbf{z}|\mathbf{x})} \log p_{\theta}(\mathbf{x}|\mathbf{z}) - D_{\text{KL}}(q_{\phi}(\mathbf{z}|\mathbf{x})||p(\mathbf{z}))] \end{aligned} \quad (1)$$

¹We adopt the definition of disentanglement and model's identifiability in [12]

As can be seen from equation (1), maximizing $\mathcal{L}(\mathbf{x}, \phi, \theta)$ will simultaneously maximize $\log p_\theta(\mathbf{x})$ and minimize $D_{\text{KL}}(q_\phi(\mathbf{z}|\mathbf{x})||p_\theta(\mathbf{z}|\mathbf{x})) \geq 0$. So, we need the $q_\phi(\mathbf{z}|\mathbf{x})$ to be flexible enough to match the true posterior $p_\theta(\mathbf{z}|\mathbf{x})$. At the same time, based on the third line of equation (1), which is often used as objective function of VAE, we require that $q_\phi(\mathbf{z}|\mathbf{x})$ is efficiently computable, differentiable, and be sampled from.

2.2 Autoregressive Normalizing Flows

Normalizing flows [21] are effective solutions to the issues mentioned above. The flow constructs flexible posterior distribution through expressing the density of $q_\phi(\mathbf{z}|\mathbf{x})$ as an expressive invertible and differentiable mapping \mathbf{g} of a random variable with a relatively simple distribution, such as an isotropic Normal. Typically, \mathbf{g} is obtained by composing a sequence of invertible and differentiable transformations $\mathbf{g}_1, \mathbf{g}_2, \dots, \mathbf{g}_K$, i.e., $\mathbf{g} = \mathbf{g}_K \circ \dots \circ \mathbf{g}_1, \mathbf{g}_k : \mathbb{R}^{d+n} \rightarrow \mathbb{R}^d, \forall k = 1 \dots K$. If we define the initial random variable (the output of encoder) as \mathbf{z}_0 and the final output random variable as \mathbf{z}_K , then $\mathbf{z}_k = \mathbf{g}_k(\mathbf{z}_{k-1}, \mathbf{x}), \forall k$. In this case, we can use \mathbf{g} to obtain the conditional probability density function of \mathbf{z}_K by applying the general probability-transformation formula [25]:

$$q_\phi(\mathbf{z}_K|\mathbf{x}) = q_\phi(\mathbf{z}_0|\mathbf{x}) |\det J_{\mathbf{g}(\mathbf{z}_0, \mathbf{x})}| \quad (2)$$

where $\det J_{\mathbf{g}(\mathbf{z}_0, \mathbf{x})}$ is the Jacobian determinants of \mathbf{g} with respect to \mathbf{z}_0 .

Autoregressive flows are one of the most popular normalizing flows [25] [22]. By carefully designing the function \mathbf{g} , the Jacobian matrix in equation (2) becomes a lower triangular matrix, so the determinant can be computed in linear time. We will only use a single-step flow as an example for illustration purposes, and still use \mathbf{g} to represent it. Multi-layer flows are simply the composition of the function represented by a single-step flow, as mentioned earlier. And we will denote the input to the function \mathbf{g} is \mathbf{z} and its output is $\tilde{\mathbf{z}}$. In the autoregressive flows, \mathbf{g} has the following form:

$$\tilde{\mathbf{z}} = \mathbf{g}(\mathbf{z}, \mathbf{x}) = [g^1(\mathbf{z}^1; \mathbf{h}^1) \dots g^1(\mathbf{z}^d; \mathbf{h}^d)]^T \quad \text{where} \quad \mathbf{h}^i = \mathbf{c}^i(\tilde{\mathbf{z}}^{<i}, \mathbf{x}) \quad (3)$$

where g^i is termed the **transformer**, a invertible function of its input \mathbf{z}^i , which is the i -th element of the vector \mathbf{z} , and \mathbf{c}^i is the i -th **conditioner**, a function of the first $i - 1$ components of $\tilde{\mathbf{z}}$, determining part of parameters of the transformer g^i . We use neural networks to fit \mathbf{c} . IAF [23] improves the performance of VAE by using an autoregressive flows, \mathbf{g} has the following form:

Performing causal inference tasks The ordering of variables in autoregressive flows can be explained using the Structural Equation Models (SEMs) framework [24], due to the similarity between equation (3) and the SEMs [26]. A special form of autoregressive flows (affine flows) allows us to obtain a new class of causal models and prove a novel causal identifiability result that generalizes additive noise models. Therefore, autoregressive flows are particularly well-suited for intervening and counterfactual queries in causal inference tasks because of their reversibility. Moreover, we could efficiently learn the causal direction between two variables or pairs of multivariate variables from a dataset by using autoregressive flows.

3 Causal Flows

Motivated by the connection between autoregressive flows and Structural Equation Models (SEMs), which provide a mean to learn the causal order among variables, we propose an extension to the autoregressive flows by incorporating an adjacency matrix A . The extended flows still involve functions with tractable Jacobian determinants.

In autoregressive flows, according to equations (3) and the third section in [24], a causal order is established among variables $\tilde{\mathbf{z}}^1, \dots, \tilde{\mathbf{z}}^d$. Given the causal graph of the variables $\tilde{\mathbf{z}}^1, \dots, \tilde{\mathbf{z}}^d$, let $A \in \mathbb{R}^{d \times d}$ denote its corresponding weighted adjacency matrix, $A_{i,:}$ is the row vector of A and $A_{i,j}$ is nonzero only if $\tilde{\mathbf{z}}^j$ is the parent node of $\tilde{\mathbf{z}}^i$, then the adjacency matrix A corresponding to the causal order in autoregressive flows is a full lower-triangular matrix. The conditioner can be written in the form of $\mathbf{c}^i(\tilde{\mathbf{z}} \circ A, \mathbf{x})$, where \circ is the element-wise product.

Let $\mathbf{I}_A = \mathbf{I}(A \neq 0)$ denote the binary adjacency matrix corresponding to A , here \mathbf{I} is the element-wise indicator function. If we utilize prior knowledge about the true causal structure among variables, i.e., if the existence of a certain causal structure(A or \mathbf{I}_A) among variables is known, then, A is still a

lower triangular matrix, but some of its elements are set to 0 according to the ground truth causal graph. We can integrate such A into the conditioner, which is also denoted as $c^i(\tilde{\mathbf{z}} \circ A, \mathbf{x})$. In the following text, we will refer to it as the **causal conditioner**.

We define autoregressive flows that use a causal conditioner as **Causal Flows**. In this framework, besides the conditioner, we also need to specify a transformer to construct the flows. The transformer can be any reversible function form, and in this paper, we focus on affine and invertible transformer, which is one of the simplest choices. At this point, the expression of flows \mathbf{g} can be formulated as follows:

$$\tilde{\mathbf{z}}^i = g^i(\mathbf{z}^i; \mathbf{h}^i) = \mathbf{z}^i \exp(s_i(\tilde{\mathbf{z}} \circ A_{i,:}, \mathbf{x})) + t_i(\tilde{\mathbf{z}} \circ A_{i,:}, \mathbf{x}) \quad (4)$$

where $\mathbf{s} = [s_1, \dots, s_d]^T \in \mathbb{R}^d$ and $\mathbf{t} = [t_1, \dots, t_d]^T \in \mathbb{R}^d$ are defined by the conditioner, i.e., $\mathbf{h}^i = \{s_i, t_i\}$, while s_1 and t_1 are constants.

Given that the derivative of the transformer with respect to \mathbf{z}^i is $\exp(s_i(\tilde{\mathbf{z}} \circ A_{i,:}))$ and A is lower-triangular matrix, the log absolute Jacobian determinant is simple to compute:

$$\log |\det J_{\mathbf{g}(\mathbf{z}, \mathbf{x})}| = \sum_{i=1}^d \log \exp(s_i(\tilde{\mathbf{z}} \circ A_{i,:}, \mathbf{x})) = \sum_{i=1}^d s_i(\tilde{\mathbf{z}} \circ A_{i,:}, \mathbf{x}) \quad (5)$$

Now, we are able to derive the log probability density function of $\tilde{\mathbf{z}}$ using the following expression:

$$\log q_{\phi}(\tilde{\mathbf{z}}|\mathbf{x}) = \log q_{\phi}(\mathbf{z}|\mathbf{x}) - \sum_{i=1}^d s_i(\tilde{\mathbf{z}} \circ A_{i,:}, \mathbf{x}) \quad (6)$$

It is worth emphasizing that the computation of autoregressive flows in equation (3) needs to be performed sequentially, meaning that $\tilde{\mathbf{z}}^{<i}$ must be calculated before $\tilde{\mathbf{z}}^i$. Due to the sampling requirement in VAE, this approach may not be as computationally efficient as the autoregressive flows represented by its inverse transformation, as demonstrated in IAF [23]. This is particularly true when dealing with high-dimensional latent variables and multiple causal flows layers. However, in causal disentanglement applications of VAE, the number of factors or latent variables of interest is often relatively small. Additionally, we've found that using a single layer of causal flows and lower-dimensional latent variables can also lead to better reconstructed image quality, as the encoder and decoder architectures play a key role in determining image quality.

4 CF-VAE: Causal Flows for VAE Disentanglement

This section focuses on addressing the issue of causal disentanglement in VAE. The main approach is to introduce causal flows into VAE, because we expect that causal flows have the same ability as autoregressive flows to learn the variable order, and further enabling VAE to learn the causal structure between its latent variables. Moreover, if the latent variables correspond to the underlying factors in the data, the final posterior distribution we obtain through causal flows can reflect the causal relationship which is similar to the connection among the corresponding factors. To this end, we will combine supervised information into the model to achieve this correspondence, ultimately achieving causal disentanglement.

It should be noted that our subsequent discussion will center on the encoder-causal flows-decoder architecture in VAEs, and we will view the encoder and flows as an unified stochastic transformation E , with the learned representation $\tilde{\mathbf{z}}$ as its final output, i.e., $\tilde{\mathbf{z}} = E(\mathbf{x})$.

First, we introduce some notations as in [12]. We denote $\xi \in \mathbb{R}^m$ as the underlying ground-truth factors of interest for data \mathbf{x} , with distribution p_{ξ} . For each underlying factor ξ^i , we denote \mathbf{y}^i as some continuous or discrete annotated observation satisfying $\mathbf{y}^i = \mathbb{E}(\xi^i|\mathbf{x})$. Let $\mathcal{D} = \{(\mathbf{x}_j, \mathbf{y}_j, \mathbf{u}_j)\}_{j=1}^N$ denotes a labeled dataset, where $\mathbf{u}_j \in \mathbb{R}^k$ is the additionally observed variable. Depending on the context, the variable \mathbf{u} can take on various meanings, such as serving as the time index in a time series, a class label, or another variable that is observed concurrently [27]. We get $\mathbf{y}^i = \mathbb{E}(\xi^i|\mathbf{x}, \mathbf{u})$, where $i = 1, \dots, m$. This is reasonable, because if \mathbf{u} is ground-truth factor \mathbf{y} , it is obviously true, otherwise, $\mathbf{y}^i = \mathbb{E}(\xi^i|\mathbf{x}, \mathbf{u}) = \mathbb{E}(\xi^i|\mathbf{x})$. Additionally, we use $\bar{E}(\mathbf{x})$ to denote the deterministic part of the stochastic transformation $E(\mathbf{x})$, i.e., $\bar{E}(\mathbf{x}) = \mathbb{E}(E(\mathbf{x})|\mathbf{x})$.

Now, we adopt the definition of causal disentanglement as follows:

Definition 1 (Disentangled representation [12]) Given the underlying factor $\xi \in \mathbb{R}^m$ of data \mathbf{x} , E is said to learn a disentangled representation with respect to ξ if there exists a one-to-one function r_i such that $\bar{E}(\mathbf{x})^i = r_i(\xi^i), \forall i = 1, \dots, m$.

As noted in [12], the purpose of this definition is to guarantee some degree of alignment between the underlying factor ξ and the latent variable $E(\mathbf{x})$ in the model. In our approach, we will also supervise each latent variable with labels for each underlying factor, thus establishing a component-wise relationship between them.

4.1 CF-VAE

To learn a disentangled representation that satisfies the above definition, we proceed to present the full probabilistic form of our CF-VAE model.

We define inference models that utilize causal flows as follows:

$$q_\phi(\mathbf{z}|\mathbf{x}, \mathbf{u}) = q_\epsilon(\mathbf{z} - \phi(\mathbf{x}, \mathbf{u})) \quad (7)$$

$$\mathbf{z} \sim q_\phi(\mathbf{z}|\mathbf{x}, \mathbf{u}) \quad (8)$$

$$\tilde{\mathbf{z}} = \mathbf{g}(\mathbf{z}, \mathbf{x}) \quad (9)$$

$$q_{\phi, \gamma}(\tilde{\mathbf{z}}|\mathbf{x}, \mathbf{u}) = q_\phi(\mathbf{z}|\mathbf{x}, \mathbf{u}) \prod_{i=1}^d \exp(-s_i(\tilde{\mathbf{z}} \circ A_{i,:}, \mathbf{x})) \quad (10)$$

where we use $\gamma = (\mathbf{s}, \mathbf{t}, A) \in \Gamma$ denotes the parameters of causal flows. Equation (7) indicates that $\mathbf{z} = \phi(\mathbf{x}, \mathbf{u}) + \epsilon$, where $p_\epsilon = \mathcal{N}(\mathbf{0}, \mathbf{I})$ and $\phi(\mathbf{x}, \mathbf{u})$ denotes the encoder. Equation (8) and (9) describe the process of transforming the original encoder output \mathbf{z} into the final latent variable representation $\tilde{\mathbf{z}}$ by using the causal flows. Eventually, equation (10) represents the posterior distribution obtained by the inference model.

Then, the conditional generative models are defined as follows:

$$p_\theta(\mathbf{x}, \tilde{\mathbf{z}}|\mathbf{u}) = p_f(\mathbf{x}|\tilde{\mathbf{z}}, \mathbf{u})p_{\mathbf{T}, \lambda}(\tilde{\mathbf{z}}|\mathbf{u}) \quad (11)$$

$$p_f(\mathbf{x}|\tilde{\mathbf{z}}) = p_f(\mathbf{x}|\tilde{\mathbf{z}}) = p_\zeta(\mathbf{x} - f(\tilde{\mathbf{z}})) \quad (12)$$

$$p_{\mathbf{T}, \lambda}(\tilde{\mathbf{z}}|\mathbf{u}) = \begin{cases} \frac{Q(\tilde{\mathbf{z}}^{\leq m})e^{<\mathbf{T}(\tilde{\mathbf{z}}^{\leq m}), \lambda(\mathbf{u})>}}{Z(\mathbf{u})} \\ \mathcal{N}(\mathbf{0}_{(d-m) \times 1}, \mathbf{I}_{(d-m) \times (d-m)}) \end{cases} \quad (13)$$

where $\theta = (f, \mathbf{T}, \lambda) \in \Theta$ are model parameters. Equation (11) describes the process of generating \mathbf{x} from \mathbf{z} . Equation (12) indicates that $\mathbf{x} = f(\tilde{\mathbf{z}}) + \zeta$, where $p_\zeta = \mathcal{N}(\mathbf{0}, \mathbf{I})$ and the decoder $f(\tilde{\mathbf{z}})$ is assumed to be an invertible function, which we approximate using a neural network. As presented in equation (13), we suggest using an exponential conditional distribution [28] for the first m dimensions and another distribution for the remaining $d - m$ dimensions (e.g., normal distribution) to capture other non-interest factors for generation [12], where $\mathbf{T} : \mathbb{R}^d \rightarrow \mathbb{R}^{d \times l}$ is the sufficient statistic, $\lambda : \mathbb{R}^k \rightarrow \mathbb{R}^{d \times l}$ is the corresponding parameter, $Q : \mathbb{R}^d \rightarrow \mathbb{R}$ is the base measure, and $Z(\mathbf{u})$ is the normalizing constant. If $d = m$, we will only use the conditional prior in the first line of (13). At this point, we can present the model architecture as shown in Figure 1.

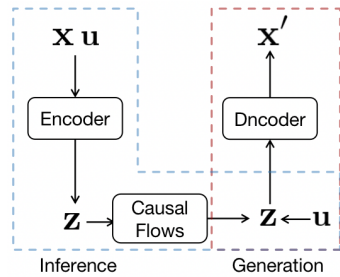


Figure 1: Model structure of CF-VAE.

By adding prior information \mathbf{u} to the prior distribution, it is no longer an independent distribution, which allows the distribution to better reflect the actual situation. Additionally, when we have label \mathbf{y} , or \mathbf{u} represents the ground-truth factors, i.e. \mathbf{y} , we can add regularization terms in the objective function to enhance the consistency between ξ and $E(\mathbf{x})$ [12] [11]. Suppose that the dataset \mathcal{X} has an empirical data distribution denoted by $q_{\mathcal{X}}(\mathbf{x}, \mathbf{u})$. Our goal turns into maximizing the variational lower bound on the marginal likelihood $p_\theta(\mathbf{x}|\mathbf{u})$.

Therefore, the loss function of **CF-VAE** is formulated as follows:

$$\begin{aligned}
\mathcal{L}(\phi, \gamma, \theta) &= -\text{ELBO}(\phi, \gamma, \theta) + \beta_{sup} \mathcal{L}_{sup}(\phi, \gamma) \\
&= \mathbb{E}_{q_{\mathcal{X}}} [\mathbb{E}_{q_{\phi, \gamma}(\tilde{\mathbf{z}}|\mathbf{x}, \mathbf{u})} \log p_{\mathbf{f}}(\mathbf{x}|\tilde{\mathbf{z}}, \mathbf{u}) - D_{\text{KL}}(q_{\phi, \gamma}(\tilde{\mathbf{z}}|\mathbf{x}, \mathbf{u})||p_{\mathbf{T}, \lambda}(\tilde{\mathbf{z}}|\mathbf{u}))] \\
&\quad + \beta_{sup} \mathbb{E}_{(\mathbf{x}, \mathbf{y}, \mathbf{u})} [l_{sup}(\phi, \gamma)]
\end{aligned} \tag{14}$$

where $\beta_{sup} > 0$ is the hyperparameter, $l_{sup}(\phi, \gamma) = \sum_{i=1}^m \mathbf{y}^i \log \sigma(\bar{E}(\mathbf{x})^i) + (1 - \mathbf{y}^i) \log (1 - \sigma(\bar{E}(\mathbf{x})^i))$ is the cross-entropy loss if \mathbf{y}^i is the binary label, and $l_{sup}(\phi, \gamma) = \sum_{i=1}^m (\mathbf{y}^i - \bar{E}(\mathbf{x})^i)^2$ is the Mean Squared Error (MSE) if \mathbf{y}^i is the continuous observation. The loss term \mathcal{L}_{sup} aligns the factor of interest $\xi \in \mathbb{R}^m$ with the first m dimensions of the latent variable \mathbf{z} , which is a technique proposed in [12] [15] to satisfy the Definition 1.

Disentanglement Identifiability Analysis Following the approach in [12], we establish the identifiability of disentanglement of CF-VAE, which confirms that our model can learn disentangled representations as defined in Definition 1. As we only focus on disentangling the factors of interest, we will, for simplicity, present our proposition in the case where $d = m$. Assumption 1 assumes that the conditional prior has sufficient capacity to contain the underlying distribution p_{ξ} , and its validity will be explained in Appendix [28] [29].

Assumption 1 *The distribution p_{ξ} belongs to the family of distributions $p_{\mathbf{T}, \lambda}$, meaning that there exists \mathbf{T}_0, λ_0 , s.t. $p_{\mathbf{T}_0, \lambda_0} = p_{\xi}$*

Proposition 1 *Under the assumptions of infinite capacity for E and \mathbf{f} , and the satisfaction of Assumption 1, the solution $(\phi^*, \gamma^*, \theta^*) \in \text{argmin}_{\phi, \gamma, \theta} \mathcal{L}(\phi, \gamma, \theta)$ of the loss function (14) guarantees that $\bar{E}_{\phi^*, \gamma^*}(\mathbf{x})$ is disentangled with respect to ξ , as defined in Definition 1.*

Proof See Appendix.

In Proposition 1, we consider the deterministic part of the posterior distribution as the learned representation, to demonstrate the disentanglement identifiability of CF-VAE.

Our model utilizes two types of supervised information: extra information \mathbf{u} and the labels \mathbf{y} of the ground-truth factors. In our experiments, we set \mathbf{u} to be the same as \mathbf{y} , so that we only need to use one type of supervised information. With the help of the supervised information, we achieve disentanglement identifiability by using the conditional prior and additional regularization terms, which also ensures the consistency between $\tilde{\mathbf{z}}^i$ and \mathbf{y}^i , and further guarantees that $\tilde{\mathbf{z}}^i$ is a causal disentangled representation, for $1 \leq i \leq m$. This means that the latent variables can capture the true underlying factors and its causal structure. The validity of our assumption 1 is explained in Appendix.

5 Related Work

Causal disentangled representation learning based on VAE In recent years, VAE models have received widespread attention for achieving causally disentangled representations due to the fact that the generative factors of real-world data are likely not independent. Authors in [17] and [18] studied disentangled causal mechanisms where the generative factors are conditionally independent, given a shared confounder. Our proposed model, in contrast, considers more general scenarios where the generative factors may exhibit more complex causal relationships.

Two main variants of the VAE for learning causally disentangled representation, CausalVAE [13] and DEAR [12], have been proposed in recent years. CausalVAE designs an SCM layer to model the causally generative mechanisms of data and has parameter identifiability using conditional priors. DEAR uses an SCM as the prior distribution of the generative model, and employs a suitable GAN algorithm to train the model while incorporating supervised information. Our model also utilizes the label of the true factors as additional supervision information to achieve disentanglement identifiability, but unlike SCM-based methods, we leverage the intrinsic properties of flows models to achieve disentanglement and do not rely on external algorithms for training.

Recently, it has been proposed that the causal relationship from the latent variable to the generated output may not hold due to the entangled structure of the decoder [19]. To make the causal relationship of the latent variable reflected in the generated output, a disentangled decoder model needs to be

trained. We believe that our model can generate images sampled from the interventional distribution, which can satisfy practical needs. Moreover, we focus on representation learning, and the disentangled representation output by the encoder is more worthy of consideration, which is also useful for downstream tasks.

Causal structure in flow models Autoregressive flows can interpret the ordering of variables in the context of SEMs. We could efficiently learn the causal direction between two variables by using it. Inspired by this, we design causal flows. In a separate parallel work, the authors of paper [30] proposed a generalized graphical normalizing flows, which serves as a general form of coupling and autoregressive flows. Similar to our design, they utilized a conditioner that integrates an adjacency matrix. However, their approach diverges from ours as we focus on developing a causal conditioner to incorporate causal structure knowledge into the flows for achieving disentanglement, inspired by the application of autoregressive flows. Instead, they explored the relationship between flows models from a Bayesian network perspective and designed a general graph conditioner primarily for better density estimation. Nevertheless, their theory also indirectly reflects the theoretical rationality of our model.

6 Experiments

We empirically evaluate CF-VAE, and demonstrate that the learned representations are causally disentangled, enabling the model to perform well on various tasks. We conducted experiments on both synthetic dataset and real human face image dataset, and compared CF-VAE with state-of-the-art VAE-based disentanglement methods. Code for reproducing our model is publicly available online.

6.1 Experimental setup

We utilize datasets where the underlying generative factors are causally related. The synthetic dataset used is the Pendulum [13], with the labels and causal graph of the factors as shown in Figure 2(a). Its labels are all continuous and the training and testing sets consist of 5847 and 1461 samples, respectively. The real human face dataset [31] is the widely used CelebA, with 40 discrete labels. We consider two sets of causally related factors [12], named CelebA(Attractive) and CelebA(Smile) with causal graphs also depicted in Figure 2(b) and 2(c). The training and testing sets consist of 162770 and 19962 samples, respectively.

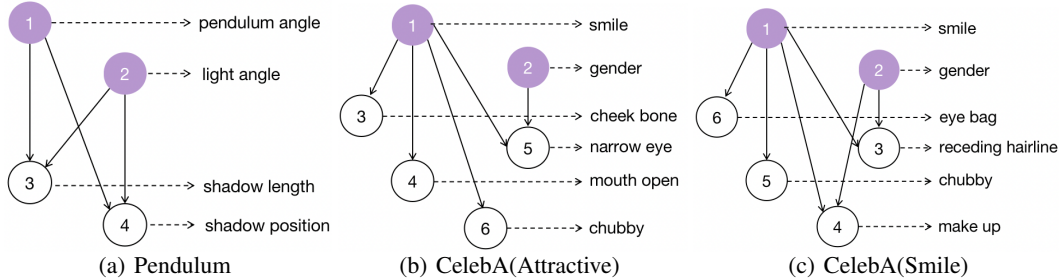


Figure 2: Causal graphs of Pendulum and CelebA. The colored circles represent the causal variables in the graphs. In Figures (a), (b), and (c), we have labeled the underlying factors we considered in each dataset.

We compare our method against several representative baseline approaches for disentanglement in VAE [2], including β -VAE [4], β -TCVAE [7], and DEAR [12]. Additionally, we compare our method to vanilla VAE [3] to highlight the advantages of disentanglement techniques. To ensure a fair comparison with equal amounts of supervised information, we use the same conditional prior and loss term with labeled data for each of these methods, as in CF-VAE. Furthermore, except for DEAR, we utilize the same encoder and decoder network structures since we consider the design of DEAR’s encoder and decoder to be part of its model innovation. For comprehensive implementation details and hyperparameters, please refer to the Appendix.

6.2 Experimental Results

Now, we proceed to evaluate our method from several aspects and provide an analysis of the corresponding experimental results.

Causally Disentangled Representation To verify that CF-VAE indeed learns disentangled representations, we conduct intervention experiments. Intervention experiments involve performing the "do- operation" in causal inference [32], which allows us to visually observe the causal disentanglement of representations. Using the single-step causal flows as an example, we demonstrate the stpdf our model takes to perform the do-operation. First, for a trained model, we input the sample \mathbf{x} into the encoder, obtaining the output \mathbf{z} . Assuming we wish to perform the "do" operation on $\tilde{\mathbf{z}}^i$, i.e., $do(\tilde{\mathbf{z}}^i = c)$, we treat equation (4) as the SCM model and set the input and output of $\tilde{\mathbf{z}}^i$ to the control value c while other values are then iteratively computed from input to output. Finally, the resulting $\tilde{\mathbf{z}}$ is decoded to generate the desired image, which corresponds to generating images from the intervened distribution of latent factor $\tilde{\mathbf{z}}$.

To verify the effectiveness of our model in achieving causal disentangled representations, we perform intervention experiments by applying the do-operation on $m - 1$ variables, resulting in only one variable's value being changed. This operation, which we refer to as "traverse", serves as a means to test the disentanglement of the model. Figures 3 and 4 show the experimental results of the CF-VAE and DEAR models on the pendulum and face datasets, respectively. We observe that when traversing a latent variable dimension, the CF-VAE model has almost only one factor changing, while the DEAR model has multiple factors changing. This is clearly shown by comparing the traversals of the third row for shadow length in Figures 3(a) and 3(b) and the second row for gender in Figures 4(a) and 4(b). Therefore, our model can better achieve causal disentanglement.

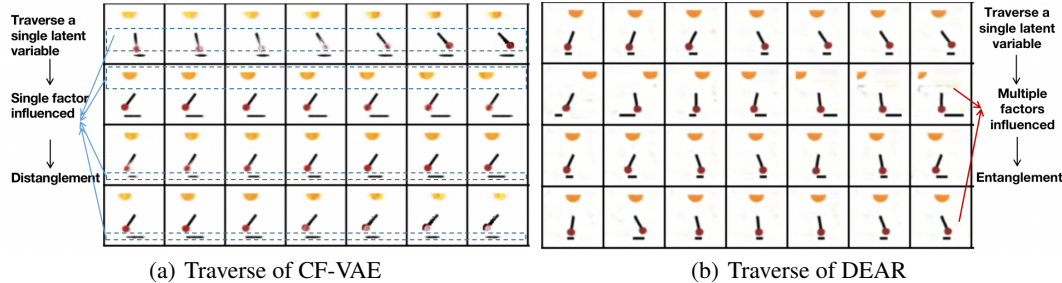


Figure 3: Results of traverse experiments on Pendulum. Each row corresponds to a variable that we traverse on, specifically, pendulum angle, light angle, shadow length, and shadow position.

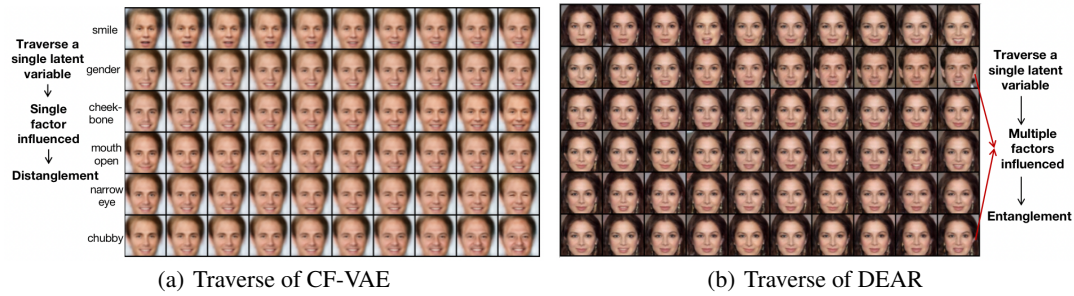


Figure 4: Results of traverse experiments on CelebA(Smile). Each row corresponds to a variable that we traverse on, specifically, smile, gender, cheek bone, mouth open, narrow eye and chubby.

To demonstrate that our model is capable of performing interventions so generating new images that do not exist in the dataset, we conduct do-operations on individual latent variables, as described earlier. As shown in Figure 5, each row corresponds to a do-operation on a single dimension. In Figure 5(a), we observe that intervening on the pendulum angle and light angle causes a change in shadow length based on physical principles, but intervening on shadow length has little effect on either of the two factors. Similarly, as shown in Figure 5(b), intervening on gender affects narrow

eye, but not vice versa. This demonstrates that intervening on the cause factor influences the effect factor, but not the other way around. This reflects that our latent variables have learned the causal structure among factors, which may be attributed to the design of the causal flows with the inclusion of variable A . With the inclusion of variable A , we are able to leverage the causal structure among true factors to enable the VAE to learn the true posterior distribution of the latent factors and achieve causal disentanglement. More traverse and intervention results are shown in the Appendix.

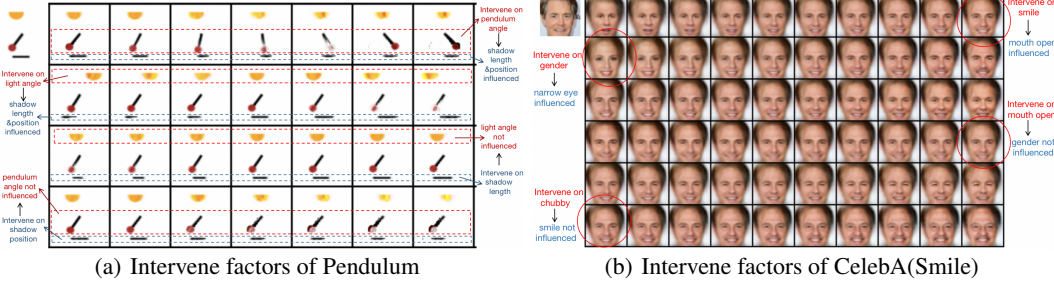


Figure 5: Results of intervention on only one variable for both Pendulum and CelebA(Smile). The image in the upper left corner of (a) and(b) are the tests data we consider respectively.

Downstream task To further illustrate the benefits of causal disentangled representation, we consider its impact on downstream tasks in terms of sample efficiency. A common downstream task is classification, and thus we choose two classification tasks to compare our model with baseline models. Firstly, for the Pendulum, we normalize the data to $[-1, 1]$ during preprocessing. Then, we manually create a classification task: if $pendulum\ angle > 0$ and $light\ angle > 0$, the target label $y = 1$; otherwise, $y = 0$. This represents a positive class if both the pendulum and light are on the right side and a negative class otherwise. For the CelebA(Attractive) dataset, we adopt the same classification task as in [12].

We employ a MLP to train classification models, where both the training and testing sets consist of the latent variable representation \tilde{z} obtained from the encoding of the input samples x , as well as their corresponding labels y . The architecture of MLP is detailed in the Appendix. We adopted the statistical efficiency score defined in [2] and [12] as a measure of sample efficiency, which is defined as the classification accuracy of 100 test samples divided by the number of all (pendulum)/10,000 test samples (CelebA). The experimental results are presented in Table 1, where we report both the test accuracy and sample efficiency.

Table 1: Test accuracy and sample efficiency of different models on the Pendulum and CelebA datasets. Mean \pm standard deviations are included in the Table.

Model	Pendulum			CelebA		
	100(%)	All(%)	Sample Eff	100(%)	10000(%)	Sample Eff
CF-VAE	99.00\pm0	99.43 \pm 0.34	99.57\pm0.34	81.00\pm1.73	81.54\pm1.76	99.34\pm0.27
DEAR	88.00 \pm 0	88.55 \pm 0.04	98.63 \pm 1.33	61.00 \pm 3.60	68.50 \pm 0	89.05 \pm 5.26
β -VAE	98.67 \pm 1.15	99.59\pm0.07	98.94 \pm 0.92	62.33 \pm 5.69	68.49 \pm 0.02	91.01 \pm 8.28
β -TCVAE	97.67 \pm 1.15	99.38 \pm 0.48	98.27 \pm 0.79	75.33 \pm 3.21	78.72 \pm 4.93	95.83 \pm 4.10
VAE	98.33 \pm 0.58	99.48 \pm 0.39	98.72 \pm 0.37	60.33 \pm 2.89	68.50 \pm 0	88.08 \pm 4.21

Table 1 shows that CF-VAE achieves the best sample efficiency and test accuracy on both datasets, except for the test accuracy of Pendulum where β -VAE is the best. However, β -VAE is significantly outperformed by CF-VAE in other accuracy metrics, especially on the complex CelebA dataset. Among the baseline models, none stand out and all perform worse than CF-VAE. It is worth noting that the encoder structures of the compared models are identical, except for DEAR, which uses ResNet as the encoder and also exhibits strong learning capacity. Therefore, we attribute the superiority of our model to our modeling approach, i.e., leveraging the fitting ability of flows, especially causal flows that greatly enhance the encoder’s ability to learn semantically meaningful representations of latent variables.

Apart from the aforementioned applications, CF-VAE has the potential to learn the true causal relationships between underlying factors, even without using a structural causal model (SCM) model [20] like [13]. As shown in Figure 7(a)-7(d), for the pendulum dataset, when our model A adopts the super-graph shown in Figure 6, though the values of A initialized randomly around 0, it gradually approaches the true causal structure with the increase of training process. If we set a threshold of 0.2, i.e., considering edges in causal graph smaller than the threshold as non-existing, we can obtain Figure 7(e), whose weighted matrix corresponds to the true causal structure. Details see Appendix.

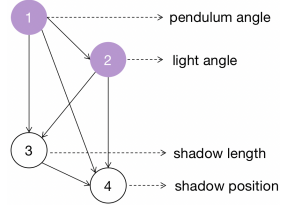


Figure 6: Super-graph of Pendulum.

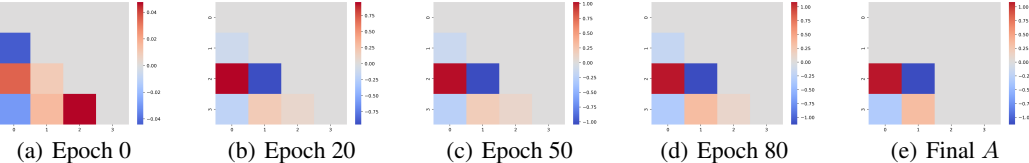


Figure 7: The learned weighted matrix A given a super-graph on Pendulum. (a)-(d) illustrate the changes in A as the training progresses. (e) represents A after threshold processing.

We also use Maximal Information Coefficient (MIC) and Total Information Coefficient (TIC) [13] [33] to measure the strength of the association between learned representations by different models and ground-truth factors. We use all the data in the testing dataset to obtain MIC and TIC. As Table 2 demonstrates, CF-VAE outperforms others on the Pendulum, while on the two CelebA datasets, CF-VAE and β -TCVAE models perform comparably. This indicates that our model achieves almost optimal correlation with the ground-truth factors compared to other baseline models, further validating the effectiveness of our learned representations. Although β -TCVAE exhibits good performance, the traverse experiments in the Appendix and the results presented in Table 1 suggest that it is possible for one latent variable to contain a variety of information, thereby leading to misleading outcomes with high correlation with many factors simultaneously.

Table 2: MIC and TIC between ground-truth factors and hidden variable representations obtained by different models on three datasets.

Model	Pendulum		CelebA(Attractive)		CelebA(Smile)	
	MIC	TIC	MIC	TIC	MIC	TIC
CF-VAE	93.27	89.90	42.38	42.09	58.53	58.60
DEAR	32.90	30.55	34.73	34.31	52.59	52.95
β -VAE	41.57	35.22	15.61	15.81	33.80	33.65
β -TCVAE	86.18	82.18	43.47	43.36	59.30	58.96
VAE	60.78	55.09	27.40	27.33	35.79	35.70

7 Conclusion

This paper focuses on learning disentangled representations with causal dependency among generative factors using VAE. To this end, we introduce causal flows that incorporate causal structure information of variables, and propose CF-VAE, a new VAE model that integrates causal flows into the encoder. By using the additional information of u and y , which can be both treated as labels of the ground-truth factors, the model achieves disentanglement identifiability. Experiments conducted on both synthetic and real datasets show that CF-VAE can achieve causal disentanglement and perform intervention experiments. Furthermore, CF-VAE exhibits excellent downstream task performance and potential to learn the causal structure. To the best of our knowledge, our approach is the first to achieve causal disentanglement without relying on SCM models, while also not restricting the generation of factor causal graphs, thereby suggesting a promising research direction in this field.

Acknowledgements

This research is supported by the National Nature Science Foundation of China under Grant 12071428 and 62111530247, and the Zhejiang Provincial Natural Science Foundation of China under Grant LZ20A010002.

References

- [1] Y. Bengio, A. Courville, and P. Vincent, “Representation learning: A review and new perspectives,” *IEEE transactions on pattern analysis and machine intelligence*, vol. 35, no. 8, pp. 1798–1828, 2013.
- [2] F. Locatello, S. Bauer, M. Lucic, G. Raetsch, S. Gelly, B. Schölkopf, and O. Bachem, “Challenging common assumptions in the unsupervised learning of disentangled representations,” in *international conference on machine learning*. PMLR, 2019, pp. 4114–4124.
- [3] D. P. Kingma and M. Welling, “Auto-encoding variational bayes,” *arXiv preprint arXiv:1312.6114*, 2013.
- [4] I. Higgins, L. Matthey, A. Pal, C. Burgess, X. Glorot, M. Botvinick, S. Mohamed, and A. Lerchner, “beta-vae: Learning basic visual concepts with a constrained variational framework,” in *International conference on learning representations*, 2017.
- [5] C. P. Burgess, I. Higgins, A. Pal, L. Matthey, N. Watters, G. Desjardins, and A. Lerchner, “Understanding disentangling in \beta-vae,” *arXiv preprint arXiv:1804.03599*, 2018.
- [6] H. Kim and A. Mnih, “Disentangling by factorising,” in *International Conference on Machine Learning*. PMLR, 2018, pp. 2649–2658.
- [7] R. T. Chen, X. Li, R. B. Grosse, and D. K. Duvenaud, “Isolating sources of disentanglement in variational autoencoders,” *Advances in neural information processing systems*, vol. 31, 2018.
- [8] A. Kumar, P. Sattigeri, and A. Balakrishnan, “Variational inference of disentangled latent concepts from unlabeled observations,” *arXiv preprint arXiv:1711.00848*, 2017.
- [9] M. Kim, Y. Wang, P. Sahu, and V. Pavlovic, “Relevance factor vae: Learning and identifying disentangled factors,” *arXiv preprint arXiv:1902.01568*, 2019.
- [10] E. Dupont, “Learning disentangled joint continuous and discrete representations,” *Advances in Neural Information Processing Systems*, vol. 31, 2018.
- [11] F. Locatello, M. Tschannen, S. Bauer, G. Rätsch, B. Schölkopf, and O. Bachem, “Disentangling factors of variation using few labels,” *arXiv preprint arXiv:1905.01258*, 2019.
- [12] X. Shen, F. Liu, H. Dong, Q. Lian, Z. Chen, and T. Zhang, “Weakly supervised disentangled generative causal representation learning,” *Journal of Machine Learning Research*, vol. 23, pp. 1–55, 2022.
- [13] M. Yang, F. Liu, Z. Chen, X. Shen, J. Hao, and J. Wang, “Causalvae: Disentangled representation learning via neural structural causal models,” in *Proceedings of the IEEE/CVF conference on computer vision and pattern recognition*, 2021, pp. 9593–9602.
- [14] I. Khemakhem, D. Kingma, R. Monti, and A. Hyvarinen, “Variational autoencoders and nonlinear ica: A unifying framework,” in *International Conference on Artificial Intelligence and Statistics*. PMLR, 2020, pp. 2207–2217.
- [15] F. Locatello, B. Poole, G. Rätsch, B. Schölkopf, O. Bachem, and M. Tschannen, “Weakly-supervised disentanglement without compromises,” in *International Conference on Machine Learning*. PMLR, 2020, pp. 6348–6359.
- [16] F. Träuble, E. Creager, N. Kilbertus, F. Locatello, A. Dittadi, A. Goyal, B. Schölkopf, and S. Bauer, “On disentangled representations learned from correlated data,” in *International Conference on Machine Learning*. PMLR, 2021, pp. 10401–10412.
- [17] R. Suter, D. Miladinovic, B. Schölkopf, and S. Bauer, “Robustly disentangled causal mechanisms: Validating deep representations for interventional robustness,” in *International Conference on Machine Learning*. PMLR, 2019, pp. 6056–6065.
- [18] A. G. Reddy, V. N. Balasubramanian *et al.*, “On causally disentangled representations,” in *Proceedings of the AAAI Conference on Artificial Intelligence*, vol. 36, no. 7, 2022, pp. 8089–8097.
- [19] S. An, K. Song, and J.-J. Jeon, “Causally disentangled generative variational autoencoder,” *arXiv preprint arXiv:2302.11737*, 2023.
- [20] J. Pearl *et al.*, “Models, reasoning and inference,” *Cambridge, UK: Cambridge University Press*, vol. 19, no. 2, 2000.
- [21] D. Rezende and S. Mohamed, “Variational inference with normalizing flows,” in *International conference on machine learning*. PMLR, 2015, pp. 1530–1538.

- [22] C.-W. Huang, D. Krueger, A. Lacoste, and A. Courville, “Neural autoregressive flows,” in *International Conference on Machine Learning*. PMLR, 2018, pp. 2078–2087.
- [23] D. P. Kingma, T. Salimans, R. Jozefowicz, X. Chen, I. Sutskever, and M. Welling, “Improved variational inference with inverse autoregressive flow,” *Advances in neural information processing systems*, vol. 29, 2016.
- [24] I. Khemakhem, R. Monti, R. Leech, and A. Hyvärinen, “Causal autoregressive flows,” in *International conference on artificial intelligence and statistics*. PMLR, 2021, pp. 3520–3528.
- [25] G. Papamakarios, E. Nalisnick, D. J. Rezende, S. Mohamed, and B. Lakshminarayanan, “Normalizing flows for probabilistic modeling and inference,” *The Journal of Machine Learning Research*, vol. 22, no. 1, pp. 2617–2680, 2021.
- [26] J. Pearl, “Causal inference in statistics: An overview,” 2009.
- [27] A. Hyvärinen and H. Morioka, “Unsupervised feature extraction by time-contrastive learning and nonlinear ica,” *Advances in neural information processing systems*, vol. 29, 2016.
- [28] L. Pacchiardi and R. Dutta, “Score matched neural exponential families for likelihood-free inference.” *J. Mach. Learn. Res.*, vol. 23, no. 38, pp. 1–71, 2022.
- [29] I. Khemakhem, R. Monti, D. Kingma, and A. Hyvärinen, “Ice-beem: Identifiable conditional energy-based deep models based on nonlinear ica,” *Advances in Neural Information Processing Systems*, vol. 33, pp. 12 768–12 778, 2020.
- [30] A. Wehenkel and G. Louppe, “Graphical normalizing flows,” in *International Conference on Artificial Intelligence and Statistics*. PMLR, 2021, pp. 37–45.
- [31] Z. Liu, P. Luo, X. Wang, and X. Tang, “Deep learning face attributes in the wild,” in *Proceedings of the IEEE international conference on computer vision*, 2015, pp. 3730–3738.
- [32] J. Pearl, *Causality*. Cambridge university press, 2009.
- [33] J. B. Kinney and G. S. Atwal, “Equitability, mutual information, and the maximal information coefficient,” *Proceedings of the National Academy of Sciences*, vol. 111, no. 9, pp. 3354–3359, 2014.